

Our study was limited to examining the resting state and did not incorporate activation procedures. Thus, our conclusions concern topography of the human brain while it is "idling" in a semistructured environment, which may itself influence regional brain activity. Further regional and sex differences may become evident when activity is measured during the performance of behavioral tasks or pharmacologic challenges. Nonetheless, the results suggest neural substrates for domains of human behavior related to both cognitive and emotional processing. They support a neurobiologic explanation of some sex differences in these behavioral dimensions and thus may help to explain sex-related differences in behavior. Individual differences within a sex and the overlap between the sexes may reflect "noise" in the measurement but perhaps, as can be tested empirically, can also be related to individual differences in sex-typical behavior.

REFERENCES AND NOTES

1. E. Maccoby and C. Jacklin, *The Psychology of Sex Differences* (Stanford Univ. Press, Stanford, CA, 1974).
2. C. Gouchie and D. Kimura, *Psychoneuroendocrinology* **16**, 323 (1991).
3. A. Campbell, *Men, Women and Aggression* (Basic Books, New York, 1993); D. W. Denno, *J. Crim. Law Criminol.* **81**, 80 (1994).
4. *DSM-III-R: Diagnostic and Statistical Manual of Mental Disorders* (American Psychiatric Association, Washington, DC, ed. 4, 1994), pp. 317-391.
5. M. Natale, R. E. Gur, R. C. Gur, *Neuropsychology* **21**, 555 (1983).
6. S. F. Witelson, *Brain* **112**, 799 (1989); A. S. Berrebi, R. H. Fitch, D. L. Ralphe, J. O. Denenberg, V. L. Friedrich, *Brain Res.* **438**, 216 (1988).
7. L. S. Allen, M. Hines, J. E. Shryne, R. A. Gorski, *J. Neurosci.* **9**, 497 (1989).
8. L. S. Allen and R. A. Gorski, *J. Comp. Neurol.* **302**, 697 (1990).
9. S. F. Witelson and D. L. Kigar, *ibid.* **323**, 326 (1992).
10. R. C. Gur et al., *Science* **217**, 659 (1982).
11. M. M. Mesulam, *Principles of Behavioral Neurology* (Davis, Philadelphia, 1985).
12. These areas are the ventro-medial temporal lobe cortices, hippocampus, amygdala, insula, orbito-frontal cortices, ventral striatum, basal forebrain, hypothalamus, certain thalamic and mesencephalic nuclei, and cingulate gyri [J. W. Papez, *Arch. Neurol. Psychiatry* **38**, 735 (1937); A. R. Damasio and G. W. Van Hoesen, in *Neuropsychology of Human Emotion* K. M. Hellman and P. Satz, Eds. (Guilford, New York, 1983), pp. 85-110].
13. K. S. Lashley, in *The Neuropsychology of Lashley*, F. A. Beach, D. O. Hebb, C. T. Morgan, H. W. Nissen, Eds. (McGraw-Hill, New York, 1960), pp. 217-255; N. Geschwind, *Brain* **88**, 237 (1965); *ibid.*, p. 535.
14. M. S. Gazzaniga, J. E. Bogen, R. W. Sperry, *Brain* **88**, 221 (1965); V. B. Mountcastle, Ed., *Interhemispheric Relations and Cerebral Dominance* (Johns Hopkins Press, Baltimore, MD, 1962); J. Levy, C. Trevarthen, R. W. Sperry, *Brain* **95**, 61 (1972).
15. M. P. Bryden and R. G. Ley, in *Neuropsychology of Human Emotion*, K. M. Hellman and P. Satz, Eds. (Guilford, New York, 1983), pp. 6-44; H. A. Sackeim, R. C. Gur, M. C. Saucy, *Science* **202**, 434 (1978); D. M. Tucker, *Psychol. Bull.* **89**, 19 (1981).
16. N. Geschwind and W. Levitsky, *Science* **161**, 186 (1968); S. F. Witelson and W. Pallie, *Brain* **96**, 641 (1973).
17. J. Risberg, *Neuropsychology* **24**, 135 (1986).
18. D. L. Shtasel et al., *Arch. Psychiatry* **48**, 1022 (1991).

19. There is evidence that such baseline measures are reproducible and can be considered to reflect a basal state [R. E. Gur et al., *ibid.* **44**, 126 (1987); E. J. Bartlett, *Psychiatry Res. Neuroimaging* **40**, 11 (1991)].
20. J. S. Karp et al., *J. Nuclear Med.* **31**, 617 (1990).
21. About 30 million counts were collected with an unrestricted axial acceptance angle and rebinned into 45 transaxial slices, 2 mm apart. The fine spatial sampling in transaxial and axial directions minimized partial volume effects and interpolation errors [J. S. Karp, M. E. Daube-Witherspoon, G. Muehlechner, *J. Cereb. Blood Flow Metab.* **11**, A38 (1991)].
22. The lumped constant of the FDG model is the steady-state ratio of the net extraction of FDG to that of glucose at constant plasma concentrations of FDG and glucose. M. E. Phelps, J. C. Mazziotta, S. C. Huang, *ibid.* **2**, 113 (1982); M. Reivich et al., *ibid.* **5**, 179 (1985).
23. S. M. Resnick, J. S. Karp, B. Turetsky, R. E. Gur, *J. Nuclear Med.* **34**, 2201 (1993).
24. S. A. Miura et al., *J. Neurosci. Res.* **27**, 500 (1990); D. E. Kuhl, E. J. Metter, W. H. Riege, M. E. Phelps, *J. Cereb. Blood Flow Metab.* **2**, 163 (1982); J. S. Perlmutter et al., *ibid.* **7**, 64 (1987).
25. The ratio between high gray and low white matter metabolism is about 1.6 for the R:WB indices (about 1.8 for the raw metabolic data), consistent with earlier PET studies (24) but considerably lower than ratios reported in 2-deoxyglucose autoradiographic studies in monkeys [C. Kennedy et al., *Ann. Neurol.*

- 12**, 33 (1982)]. PET does not approximate the spatial resolution of autoradiography, ROIs contain mixtures of tissue types, and values are attenuated by partial volume effects and residual scatter.
26. C. D. Spielberger, R. L. Gorsuch, R. E. Lushene, *Manual for the State-Trait Anxiety Inventory* (Consulting Psychologists Press, Palo Alto, CA, 1970).
27. These effects could likewise not be explained by sex differences in brain volume or body mass. Metabolism did not correlate with brain volume: for the whole sample, the correlation coefficient $r(59) = 0.06$, for men $r(35) = 0.14$ and for women $r(22) = 0.20$; for body mass index (mass:height²), $r = -0.05, -0.07$, and -0.02 , respectively, none of which is significant. Our sample did show a "sex-typical" pattern of performance on cognitive tests, with men outperforming women in verbal tasks and with women doing better on abstraction and verbal memory tasks.
28. A. Kertesz, M. Polk, S. Black, J. Howell, *Brain Res.* **530**, 40 (1990).
29. B. S. Peterson et al., *Magn. Reson. Imaging.* **11**, 493 (1993).
30. We thank P. Cowell, R. Erwin, K. Hambrose, L. Harris, P. Herscovitch, D. Kareken, M.-M. Mesulam, H. Mitchell-Sears, R. Petty, D. Ragland, E. Reiman, D. Sandefur, D. Shtasel, R. Smith, T. Thew, E. Zarahn, and the PET Center staff. Supported by NIH grants MH-43880, MH-42191, MH-48539, NS-14867, MH-00586, and MO1RR0040.

21 July 1994; accepted 22 November 1994

Cloning of an Intrinsic Human TFIID Subunit That Interacts with Multiple Transcriptional Activators

Cheng-Ming Chiang and Robert G. Roeder*

TFIID is a multisubunit protein complex comprised of the TATA-binding protein (TBP) and multiple TBP-associated factors (TAFs). The TAFs in TFIID are essential for activator-dependent transcription. The cloning of a complementary DNA encoding a human TFIID TAF, TAF_{II}55, that has no known homolog in *Drosophila* TFIID is now described. TAF_{II}55 is shown to interact with the largest subunit (TAF_{II}230) of human TFIID through its central region and with multiple activators—including Sp1, YY1, USF, CTF, adenoviral E1A, and human immunodeficiency virus-type 1 Tat proteins—through a distinct amino-terminal domain. The TAF_{II}55-interacting region of Sp1 was localized to its DNA-binding domain, which is distinct from the glutamine-rich activation domains previously shown to interact with *Drosophila* TAF_{II}110. Thus, this human TFIID TAF may be a co-activator that mediates a response to multiple activators through a distinct mechanism.

The multisubunit protein complex TFIID (1-5) is required for transcription by most, if not all, promoters targeted by RNA polymerase II (class II promoters). At TATA-containing class II promoters, TFIID first binds to the TATA box and then recruits other basal factors and RNA polymerase II to the promoter (6, 7). Whereas the TBP subunit is sufficient for basal transcription, activator-dependent transcription requires the TAFs of TFIID as well as upstream stimulatory activity (USA)-derived cofactors (5, 6, 8). The possibility that individual TAFs may have activator-specific func-

tions is suggested by their multiplicity (up to 8 in *Drosophila* and 13 in human TFIID) (1-5) and by the demonstration of *Drosophila* TAF-specific interactions with the mammalian activators Sp1 and Gal4-VP16 (9, 10).

The human TFIID subunit TAF_{II}55 was isolated from a cell line that expresses epitope-tagged TBP for the immunopurification of TFIID (5). Two peptide sequences derived from thermolysin digestion of TAF_{II}55 were used to design degenerate primers for polymerase chain reaction (PCR) amplification (11). The PCR product was used as a probe to screen a human placental complementary DNA (cDNA) library. A clone that contained a cDNA insert of a size corresponding to that of the

Laboratory of Biochemistry and Molecular Biology, Rockefeller University, New York, NY 10021, USA.

*To whom correspondence should be addressed.

55-9 cells and with bacterially expressed f:55 (Fig. 2A, lanes 7 and 8). The lower band corresponds to the untagged TAF_{II}55 detected in HeLa cell nuclear extracts, in the HeLa cell P11 0.85 M KCl fraction, and in f:TFIID purified from a FLAG-tagged TBP-expressing cell line (3-10), as well as to bacterially expressed untagged TAF_{II}55 (Fig. 2A, lanes 9 to 12). The protein composition of f:TFIID purified from both 55-9 and 3-10 cells was further examined by silver staining and by immunoblotting with antibodies prepared against recombinant human TAFs (TAF_{II}230, TAF_{II}135, TAF_{II}95, TAF_{II}80, TAF_{II}55, TAF_{II}43, and TAF_{II}20) (Fig. 2B). The presence of defined TAFs in both preparations indicates that TAF_{II}55 is an intrinsic TFIID subunit. The functional identity of f:TFIID purified from 55-9 cells was confirmed by transcriptional assays (14) with highly purified TFIIA, TFIIE/F/H, the cofactor fraction USA (15), RNA polymerase II, and recombinant TFIIB and Gal4-VP16. The addition of f:TFIID purified from either 3-10 or 55-9 cells supported roughly equivalent levels of both basal (Fig. 2C, lanes 2 and 7) and activated (Fig. 2C, lanes 4 and 10) transcription at comparable concentra-

tions, demonstrating the functional equivalence of both TFIID preparations.

To examine the protein-protein interactions within the TFIID complex, we expressed several NH₂-terminal and COOH-terminal deletion forms of TAF_{II}55 in bacteria (16) with the FLAG-tagged protein strategy to facilitate the purification and characterization of different interaction domains (Fig. 3, A and B). Protein blot analysis with ³²P-labeled baculovirus-expressed f:55 (17) as a probe revealed a direct interaction between TAF_{II}55 and TAF_{II}230 (Fig. 3D, left panel), the large subunit of TFIID, which has been implicated in the regulation of cell cycle progression (18, 19). Despite high backgrounds, this TAF_{II}55-TAF_{II}230 interaction was also observed in the crude TFIID (HeLa P11, 0.85 M KCl) fraction and in HeLa nuclear extracts. Consistent with previous results (3, 18, 20), TBP showed a direct interaction with TAF_{II}230 in similar assays (Fig. 3D, right panel). Solution interactions between TAF_{II}55 and TAF_{II}230 were also monitored by immunoblotting [with TAF_{II}230 and hemagglutinin (HA) antibodies] after incubation of an insect cell lysate containing

recombinant HA-tagged human TAF_{II}230 with various immobilized f:55 deletion proteins (21) (Fig. 3C). The TAF_{II}230-interacting domain was mapped to the central region of TAF_{II}55 between amino acids 139 and 249 (Fig. 3, A and C).

Because TAF_{II}55 is a highly charged protein that may potentially interact with various molecules, we explored the interactions of activators with TAF_{II}55. Interactions between affinity-purified transcription factors (22) (Fig. 4A, top panel) and TAF_{II}55 were monitored first by protein blot analysis with the ³²P-labeled baculovirus-expressed f:55 as a probe (Fig. 4A, bottom panel). Signals were detected in lanes that contained USF, Sp1, YY1, human immunodeficiency virus-type 1 (HIV-1) Tat, Gal4-E1A, and Gal4-Pro (the underloaded USF and Gal4-Pro signals are more evident in longer exposures; see also Fig. 4B), indicating a direct interaction between TAF_{II}55 and these activators; in contrast, no signal was apparent, even after longer exposure, in lanes containing equivalent amounts of HPV-11 E2, the nuclear factor κB (NF-κB) p50 subunit, LBP1c, Gal4-VP16, and the overloaded protein size

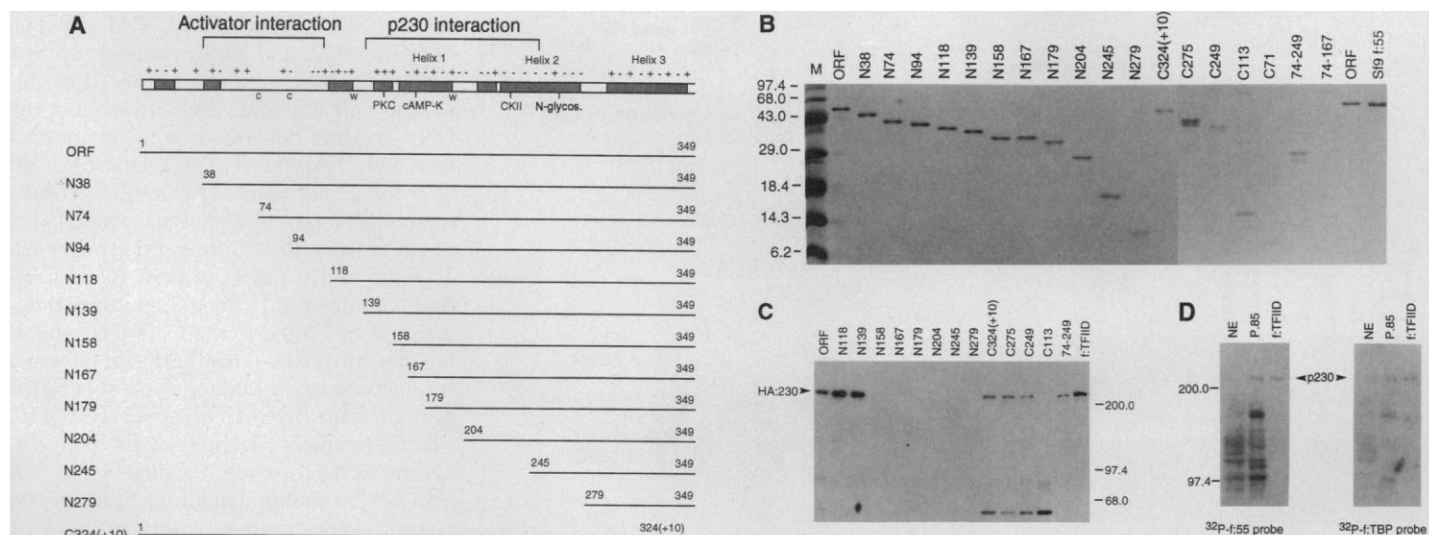


Fig. 3. The central region of TAF_{II}55 interacts with the largest subunit of TFIID. **(A)** The schematic representation of TAF_{II}55 was based mainly on computer analysis, except for the summary of the interaction studies. Potential phosphorylation sites for protein kinase C (PKC), adenosine 3',5'-monophosphate-dependent protein kinase (cAMP-K), and casein kinase II (CKII) are indicated, as are an N-glycosylation site (N-glycos.), charged (+ or -), cysteine (C), and tryptophan (W) residues, and predicted helix regions (shaded boxes). Numbers in the deletion clones denote, respectively, the first and the last residues after the NH₂- and COOH-terminal deletions. C324(+10) contains the NH₂-terminal 324 amino acids of TAF_{II}55 followed by 10 residues derived from the cloning linker sequence. All clones have the FLAG epitope sequence at the NH₂-terminus. **(B)** Coomassie blue staining of f:55 deletion proteins. The FLAG-tagged proteins were purified as described (28), without the addition of rifampicin. Two microliters of each purified protein was subjected to electrophoresis in a 12% SDS-polyacrylamide gel, which was then stained with Coomassie blue. Sizes (in kilodaltons) of prestained protein markers (M) (BRL) are indicated on the left. The lane labeled Sf9 f:55 contains f:55 purified from Sf9 cells. **(C)** Solution interaction studies with immobilized f:55 deletion proteins and an insect cell lysate containing baculovirus-expressed HA-tagged human TAF_{II}230 (HA:230). Immunoblotting was performed with polyclonal antibodies to TAF_{II}230 (2294). Similar results were obtained with monoclonal antibodies (12CA5) to the HA epitope (12). **(D)** Protein blot analysis with ³²P-labeled f:55 and f:TBP probes. The baculovirus-expressed f:55 and the bacterially expressed f:TBP (28) proteins were labeled in vitro with heart muscle kinase and [γ -³²P]ATP. Protein blotting was performed as described (30). Ten microliters of HeLa nuclear extracts (NE), P11 0.85 M KCl fraction (P. 85), and FLAG-purified TFIID (f:TFIID) from 3-10 cells was loaded onto each lane.

the last residues after the NH₂- and COOH-terminal deletions. C324(+10) contains the NH₂-terminal 324 amino acids of TAF_{II}55 followed by 10 residues derived from the cloning linker sequence. All clones have the FLAG epitope sequence at the NH₂-terminus. **(B)** Coomassie blue staining of f:55 deletion proteins. The FLAG-tagged proteins were purified as described (28), without the addition of rifampicin. Two microliters of each purified protein was subjected to electrophoresis in a 12% SDS-polyacrylamide gel, which was then stained with Coomassie blue. Sizes (in kilodaltons) of prestained protein markers (M) (BRL) are indicated on the left. The lane labeled Sf9 f:55 contains f:55 purified from Sf9 cells. **(C)** Solution interaction studies with immobilized f:55 deletion proteins and an insect cell lysate containing baculovirus-expressed HA-tagged human TAF_{II}230 (HA:230). Immunoblotting was performed with polyclonal antibodies to TAF_{II}230 (2294). Similar results were obtained with monoclonal antibodies (12CA5) to the HA epitope (12). **(D)** Protein blot analysis with ³²P-labeled f:55 and f:TBP probes. The baculovirus-expressed f:55 and the bacterially expressed f:TBP (28) proteins were labeled in vitro with heart muscle kinase and [γ -³²P]ATP. Protein blotting was performed as described (30). Ten microliters of HeLa nuclear extracts (NE), P11 0.85 M KCl fraction (P. 85), and FLAG-purified TFIID (f:TFIID) from 3-10 cells was loaded onto each lane.

markers (Fig. 4A, bottom panel). The difference in signal intensity among various activators may have been attributable to variations in amounts loaded, renaturation efficiencies, or intrinsic binding affinities for TAF_{II}55. The use of TFIIB as a probe for protein blot analysis with the same activators showed strong signals detected in lanes containing Sp1, YY1, and Gal4-VP16 (12), indicating a direct interaction between TFIIB and these activators (23). The observation that Gal4-E1A and Gal4-VP16 share the same DNA-binding domain but interact, respectively, with TAF_{II}55 and TFIIB

suggests that different activation domains may have preferential targets in the general transcriptional machinery in order to activate transcription. Interaction between TAF_{II}55 and Gal4-Pro also implies that TAF_{II}55 may associate directly with natural CTF proteins. To confirm these results for natural cellular activators, we incubated nuclear extracts with several immobilized f:55 deletion proteins and monitored bound proteins by immunoblotting with specific antibodies. This experiment confirmed interactions between TAF_{II}55 and USF, Sp1, YY1, and CTF (Fig. 4B, lanes ORF and Refer-

ence). These interactions were eliminated by NH₂-terminal deletions that extend to residue 117, but persisted (and in the case of YY1 were slightly enhanced) with COOH-terminal deletions that extend to position 114 (Fig. 4B, compare lanes ORF, N118, and C113). A more detailed mapping of the TAF_{II}55 interaction domain suggested that the NH₂-terminal region of TAF_{II}55 between amino acids 38 and 113 is essential for activator interactions (Fig. 4C). As inferred from protein blot analysis, no interaction of TAF_{II}55 with the NF- κ B p50 subunit (Fig. 4B) or LBP1c (12) was observed in solution interaction studies, indicating the specificity in these assays. The importance of the NH₂-terminal region of TAF_{II}55 in mediating interactions with HIV-1 Tat was confirmed by yeast two-hybrid analysis (12).

To further investigate TAF_{II}55-activator interactions, we mapped the TAF_{II}55-interacting domain of Sp1. The cytosolic fractions of HeLa cells infected by vaccinia viruses overexpressing either the full-length or various mutated Sp1 proteins were incubated, separately, with immobilized-TAF_{II}55 columns. Bound proteins were then eluted and detected by immunoblotting with Sp1 antibodies. All proteins that contained the COOH-terminal 168 amino acids of Sp1 interacted with TAF_{II}55 (Fig. 4D, lanes 5, 7, and 8). In contrast, an Sp1 derivative that contained only the glutamine-rich activation domains without the DNA-binding domain showed no interaction with TAF_{II}55 (Fig. 4D, lane 6), even after longer exposure. This result is consistent with protein blot analysis, which failed to show any direct interaction between TAF_{II}55 and a fusion protein (Gal4-Gln) that contained only the glutamine-rich domains of Sp1 fused to the Gal4 DNA-binding domain (12). This TAF_{II}55 targeting through the DNA-binding domain of Sp1 is distinct from that of *Drosophila* TAF_{II}110, which interacts strongly with the glutamine-rich activation domains of Sp1 (9). The DNA-binding domain of Sp1 has previously been shown to interact with YY1 (24) and with adenoviral E1A protein (25). Other examples of regulatory protein interactions with the DNA-binding domains of transcription factors include interactions of VP16 with Oct1, TBP with c-Rel, and E1A with various activators (25, 26). Attempts to assemble TFIID *in vivo* by the establishment of cell lines expressing various epitope-tagged TAF_{II}55 deletion proteins were not successful (12), possibly because of the inability of mutated TAF_{II}55 to compete with the wild-type endogenous TAF_{II}55 for assembly into TFIID complexes. Nevertheless, in corresponding cell lines, TAF_{II}55 mutants with short NH₂-terminal deletions, such as N74 and N94 (Fig. 3A), still bind TAF_{II}230, whereas

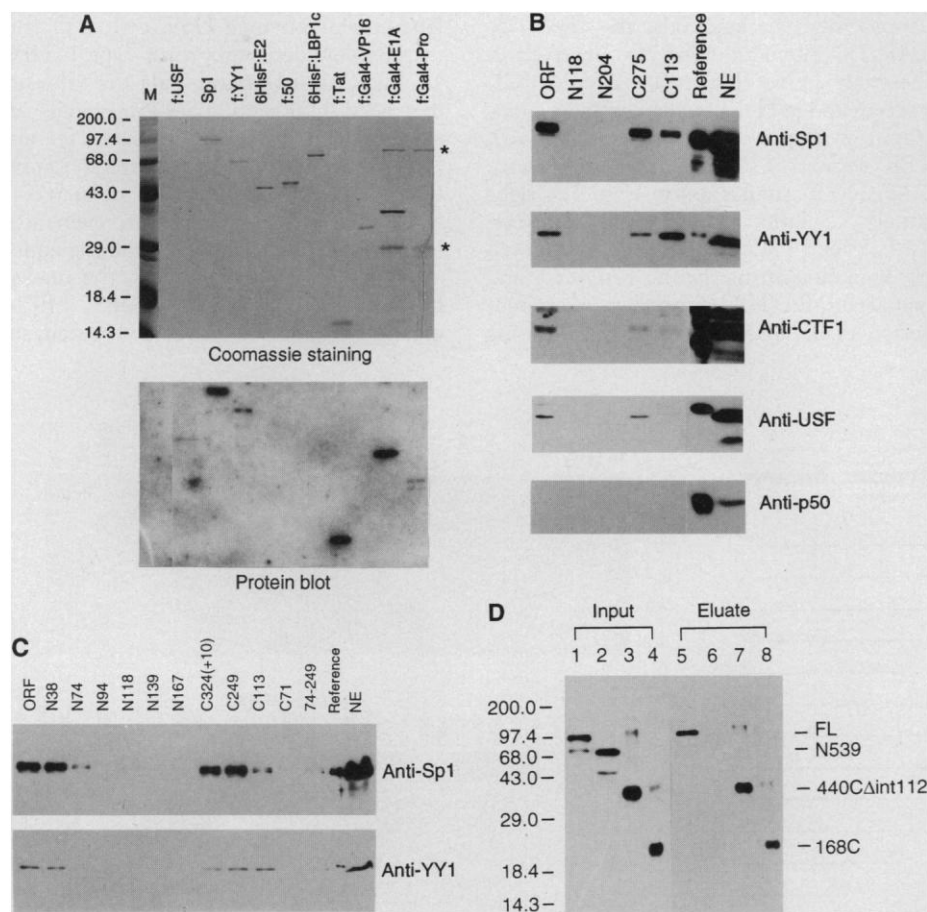


Fig. 4. TAF_{II}55-activator interactions. **(A)** TAF_{II}55 interacts with multiple transcriptional activators. (Top panel) A Coomassie blue-stained gel showing the amounts of different activators loaded. (Bottom panel) Protein blot analysis with ³²P-labeled baculovirus-expressed f:55. Asterisks denote positions of contaminant proteins copurified with Gal4 fusion proteins. M, molecular size markers. **(B)** The NH₂-terminal domain of TAF_{II}55 interacts with various activators. HeLa nuclear extracts were incubated, separately, with five different immobilized f:55 deletion proteins. The bound proteins subsequently eluted from the columns were detected by immunoblotting with specific activator antibodies. The Sp1 antibodies were from Santa Cruz. The input HeLa nuclear extracts (NE) and purified activators (22) (Reference) were also loaded, individually, as positive controls for each panel. **(C)** The NH₂-terminal region of TAF_{II}55 between amino acids 38 and 113 is essential for interaction with various activators. Solution interaction studies were performed with various immobilized f:55 deletion proteins and HeLa nuclear extracts as described in (B). **(D)** TAF_{II}55 interacts with the DNA-binding domain of Sp1. The cytosolic fractions of HeLa cells infected by vaccinia viruses that overexpress various Sp1 proteins—including the full-length protein (FL), the NH₂-terminal 539 residues that contain both the glutamine-rich activation domains A and B (N539), activation domain B linked to the COOH-terminal 168 residues (440C Δ int112), and the COOH-terminal 168 residues containing the DNA-binding domain and the activation domain D (168C) (32)—were incubated, separately, with columns of immobilized full-length TAF_{II}55 that was prepared with the use of the FLAG tag. Bound proteins were then eluted and detected by immunoblotting with Sp1 antibodies. Molecular sizes (in kilodaltons) of the prestained protein markers are indicated on the left.

TAF_{II}55 mutants with a deletion to residue 166 show no interaction with TAF_{II}230 (12). These results further strengthen the conclusion of the TAF_{II}55 and TAF_{II}230 interaction studies based on *in vitro* solution interaction assays (Fig. 3C).

Previous studies have shown interactions of *Drosophila* TAF_{II}110 and *Drosophila* TAF_{II}40 with the glutamine-rich activation domains of human Sp1 and the acidic activation domain of Gal4-VP16, respectively, which suggests that individual TAFs may serve as targets for different types of activation domains (9, 10). We have shown here that a single human TFIID TAF (TAF_{II}55) with no apparent *Drosophila* homolog is capable of interacting with a variety of mammalian activators whose activation domains and DNA-binding domains are thought to differ in overall character but could share subtle commonality of structure (27). In the case of Sp1 (Fig. 4D) and USF (12), it appears that targeting to the DNA-binding domain of activators by a TFIID TAF may be another way to modulate transcriptional activities. Given the restricted number of TAFs in TFIID, and assuming that they help mediate activation by the hundreds of activators so far identified, it seems reasonable, on the basis of our results, that a single TAF may serve as a target for multiple transcriptional activators. The observation that some activators can interact with multiple components (basal factors, TAFs, or USA-derived cofactors) in the transcriptional machinery is consistent either with concerted (possibly synergistic) interactions of multiply bound activators (or distinct domains in a single activator) or with sequential or alternative interactions of a single activator on a given promoter (8).

REFERENCES AND NOTES

- B. D. Dynlacht, T. Hoey, R. Tjian, *Cell* **66**, 563 (1991); B. F. Pugh and R. Tjian, *Genes Dev.* **5**, 1935 (1991); T. Kokubo *et al.*, *J. Biol. Chem.* **268**, 17554 (1993).
- N. Tanese, B. F. Pugh, R. Tjian, *Genes Dev.* **5**, 2212 (1991).
- R. Takada *et al.*, *Proc. Natl. Acad. Sci. U.S.A.* **89**, 11809 (1992).
- Q. Zhou, P. M. Lieberman, T. G. Boyer, A. J. Berk, *Genes Dev.* **6**, 1964 (1992).
- C.-M. Chiang, H. Ge, Z. Wang, A. Hoffmann, R. G. Roeder, *EMBO J.* **12**, 2749 (1993).
- R. G. Roeder, *Trends Biochem. Sci.* **16**, 402 (1991).
- L. Zawal and D. Reinberg, *Curr. Opin. Cell Biol.* **4**, 488 (1992); R. C. Conaway and J. W. Conaway, *Annu. Rev. Biochem.* **62**, 161 (1993).
- H. Ge and R. G. Roeder, *Cell* **78**, 513 (1994); M. Kretschmar, K. Kaiser, F. Lottspeich, M. Meisterernst, *ibid.*, p. 525.
- T. Hoey *et al.*, *ibid.* **72**, 247 (1993).
- J. A. Goodrich, T. Hoey, C. J. Thut, A. Admon, R. Tjian, *ibid.* **75**, 519 (1993).
- The thermolysin digestion of the TAF_{II}55 protein bound to a polyvinylidene difluoride membrane was performed as described [J. Fernandez, M. DeMott, D. Atherton, S. M. Mische, *Anal. Biochem.* **201**, 255 (1992)]. The first two peptide sequences shown in Fig. 1 were used to design two degenerate primers, 5'-ACIATIGA(A/G)CTIC(A/C/T)CCIGATGGICGICATGGIATIGTICGIGTIG(A/C/T)-3' and 5'-TG(A/V)TC(T/C)TCIGCIATAT(T/C)TCICCGIGTGGAIACIGCITCIGCATCIGT-3', for PCR amplification of single-stranded cDNA that was derived from polyadenylated RNA of human cervical carcinoma C-33A cells by reverse transcription-PCR [C.-M. Chiang, L. T. Chow, T. R. Broker, *Methods Mol. Biol.* **15**, 189 (1993)]. The PCR product was then used to screen a human placental cDNA library [M. Hirata *et al.*, *Nature* **349**, 617 (1991)]. Seven positive clones were isolated from 10⁶ phage plaques; three have G, whereas the other four have T, at nucleotide 1224. The second peptide sequence obtained has a serine residue at this particular position.
- C.-M. Chiang and R. G. Roeder, unpublished data.
- The bacterial expression plasmids pF:55-11d and p55-11a express the FLAG-tagged and untagged TAF_{II}55, respectively. An Nde I site was first created by PCR at the initiation codon of the TAF_{II}55 cDNA, which was rescued in pBS-SK(-) from the 7-21 lambda Zapll phage isolate (Stratagene). The fragment between this Nde I site and a Bam HI site (located at the downstream linker sequence) of TAF_{II}55 cDNA (containing nucleotides 691 to 2274) was then cloned into pF:TBP-11d (28), after removal of the TBP insert by Nde I and Bam HI digestion, to create pF:55-11d. In a similar manner, the TAF_{II}55 open reading frame was isolated from pF:55-11d at the Nde I and Bam HI sites (created at the termination codon of TAF_{II}55) and cloned into pET-11a (Novagen) to create p55-11a. The plasmid pBn-F:55 was constructed by cloning the TAF_{II}55 cDNA from pF:55-11d after Bam HI and partial Bgl II digestion into the Bam HI site of pBabe neo [J. P. Morgenstern and H. Lund, *Nucleic Acids Res.* **18**, 3587 (1990)]; it was used to establish 55-9 cells by retrovirus-mediated gene transfer as described (5).
- Purification of TFIIA, TFIIE/F/H, and USA from 3-10 nuclear extracts was as described for HeLa cells (5). Purification of RNA polymerase II from 3-10 nuclear pellets, recombinant Gal4-VP16, and FLAG-tagged TFIIB was according to the published procedures (28, 29) [D. Reinberg and R. G. Roeder, *J. Biol. Chem.* **262**, 3310 (1987)]. Transcriptional assays were performed as described (5).
- M. Meisterernst, A. L. Roy, H. M. Lieu, R. G. Roeder, *Cell* **66**, 981 (1991).
- All of the f:55 deletion plasmids, except C324(+10) and C113, were constructed by introducing either Nde I or Bam HI sites by PCR at the NH₂-terminus- or COOH-terminus-encoding sequences of deletion clones. The Nde I and Bam HI fragments of different deletion clones were then swapped with the full-length TAF_{II}55 clone pF:55(ORF)-11d, which has Nde I and Bam HI sites created respectively at the initiation and termination codons of the wild-type TAF_{II}55 cDNA (nucleotides 691 to 1740). C324(+10) and C113 were created by insertion of a translational termination linker (5'-CTAGACTAGTCTAGCTCGA-GGATCCTAGGTAGC-3') into the Sac I and Nhe I sites, separately, of pF:55(ORF)-11d after blunt-end ligation.
- We constructed the baculoviral expression plasmid pVL-F:55 by cloning the Bam HI-Xba I fragment of pGEM7-F:55 into pVL1393 (Invitrogen) at the same enzyme cutting sites. We created the plasmid pGEM7-F:55 by inserting the Nde I-Xba I fragment of pF:55-11d (spanning nucleotides 691 to 2045) into pFLAG(AS)-7 (5) after Nde I and Xba I digestion. Recombinant baculoviruses expressing f:55 were generated by cotransfecting 1 μg of pVL-F:55 and 0.25 μg of BaculoGold linearized baculoviral DNA (PharMingen) into Sf9 insect cells with 10 μl of cationic liposome (Invitrogen) and 0.5 ml of TC-100 (Gibco). The baculovirus-expressed f:55 was purified from the Sf9 cell pellets 48 hours after viral infection with the same procedures used for purification of the bacterially expressed f:55 (Fig. 2). Two hundred nanograms of purified f:55 and f:TBP were labeled with ³²P at the heart muscle kinase phosphorylation site present in the FLAG-tagged sequence (28, 30) by incubation with heart muscle kinase and [γ -³²P]ATP (adenosine triphosphate) for 30 min at 30°C. Labeled proteins were then separated from the unincorporated free nucleotide with the Nick column (Pharmacia) and used as probes for protein blot analysis as described (30).
- S. Ruppert, E. H. Wang, R. Tjian, *Nature* **362**, 175 (1993); K. Hisatake *et al.*, *ibid.*, p. 179.
- E. H. Wang and R. Tjian, *Science* **263**, 811 (1994).
- Q. Zhou, T. G. Boyer, A. J. Berk, *Genes Dev.* **7**, 180 (1993); T. Kokubo *et al.*, *ibid.*, p. 1033; R. O. J. Weinzierl, B. D. Dynlacht, R. Tjian, *Nature* **362**, 511 (1993).
- Sf9 insect cells were harvested 48 hours after infection with recombinant baculoviruses carrying the human HA:230 gene. Cell pellets were resuspended in bacterial lysis buffer (28) containing 0.1% NP-40, sonicated to break cells, and centrifuged. The supernatant was then incubated with different f:55 deletion proteins immobilized in M2 agarose (IBI/Kodak). The bound proteins were recovered after elution with the synthetic FLAG peptide (28) and used for immunoblot analysis.
- Sp1 was purified from HeLa cells by wheat germ agglutinin and oligonucleotide columns as previously described [S. P. Jackson and R. Tjian, *Proc. Natl. Acad. Sci. U.S.A.* **86**, 1781 (1989)]. The other activators were expressed in and purified from bacteria after introducing an Nde I site by PCR at the initiation codon of each cDNA and cloning into the FLAG-expression plasmids. Briefly, pF:USF-11d, pF:YY1-11d, p6HisF:E2-11d, pF:50-11d, p6HisF:LBP1c-11d, pF:Tat-11d, pF:Gal4-VP16, pF:Gal4-E1A, pF:Gal4-Pro, and pF:Gal4-Gln are individual expression plasmids for FLAG-tagged USF, YY1, HPV-11 E2, NF-κB p50, LBP1c, HIV-1 Tat, Gal4-VP16, Gal4-E1A, Gal4-Pro, and Gal4-Gln, which were constructed, respectively, from pET3dUSF [H. Kaulen, P. Pogononec, P. D. Gregor, R. G. Roeder, *Mol. Cell Biol.* **11**, 412 (1991)], pGEM7Z(+)-14.1 [Y. Shi, E. Seto, L.-S. Chang, T. Shenk, *Cell* **67**, 377 (1991)], pCMV-E2 [C.-M. Chiang *et al.*, *Proc. Natl. Acad. Sci. U.S.A.* **89**, 5799 (1992)], p50-pBS+ [T. Fujita, G. P. Nolan, S. Ghosh, D. Baltimore, *Genes Dev.* **6**, 775 (1992)], 11K-LBP1c [J.-B. Yoon, G. Li, R. G. Roeder, *Mol. Cell Biol.* **14**, 1776 (1994)], pcTat [M. H. Malim, J. Hauber, R. Fenrick, B. R. Cullen, *Nature* **335**, 181 (1988)], pGal4-VP16 [I. Sadowski, J. Ma, S. Triezenberg, M. Ptashne, *ibid.*, p. 563], pGal4-E1A (2), pGal4-Pro (2), and pGal4-Gln (2) between the created Nde I site at the initiation codon and the downstream Bam HI (for USF, YY1, p50, LBP1c, Tat, and Gal4-VP16) or Xho I (E2, Gal4-E1A, Gal4-Pro, and Gal4-Gln; the last three clones were constructed by blunt-end ligation after Xba I and Klenow digestion) sites. The plasmid p6HisF-11d has both six histidine and FLAG tags to facilitate protein purification under different conditions, and it was created by cloning a synthetic linker (5'-TATCGACTACAGACGATGACGATAAAGCAAGAAGAGCATCTGTGCA-3' and 5'-TATGACACAGATGCTCTTGCTTTATGCTGCA-TCGTCTTTGTAGTCGA-3') into pET-15b (Novagen) at the Nde I site. For purification of FLAG-tagged Gal4 fusion proteins, bacterial cultures containing individual plasmids were induced and harvested as previously described for regular FLAG-tagged proteins (28). Bacterial pellets from 1-liter cultures were resuspended in 30 ml of buffer A (29) containing 0.4 M NaCl and 0.1% NP-40, and sonicated to break cells. A portion (10 ml) of the sonication supernatant was incubated overnight with 200 μl of M2 agarose. The M2 agarose with bound proteins was washed four times in buffer A containing 0.4 M NaCl and four times in BC100/Zn buffer [20 mM tris-Cl (pH 7.9 at 4°C), 20% (v/v) glycerol, 10 μM zinc acetate, 100 mM KCl, 0.5 mM phenylmethylsulfonyl fluoride, and 1 mM dithiothreitol], and finally transferred to a microcentrifuge spin column (Invitrogen). The bound proteins were then eluted from the M2 agarose by incubation with 400 μl of BC100/Zn containing 0.2 mg of the FLAG peptide at 4°C for 1 hour. Purification of the other FLAG-tagged proteins was as described (28), without the addition of rifampicin.
- Y.-S. Lin and M. R. Green, *Cell* **64**, 971 (1991); A. Usheva and T. Shenk, *ibid.* **76**, 1115 (1994).
- J.-S. Lee, K. M. Galvin, Y. Shi, *Proc. Natl. Acad. Sci. U.S.A.* **90**, 6145 (1993).
- F. Liu and M. R. Green, *Nature* **368**, 520 (1994).
- S. Stern, M. Tanaka, W. Herr, *ibid.* **341**, 624 (1989); L. D. Kerr *et al.*, *ibid.* **365**, 412 (1993).
- W. D. Cress and S. J. Triezenberg, *Science* **251**, 87 (1991); J. L. Regier, F. Shen, S. J. Triezenberg, *Proc.*

- Natl. Acad. Sci. U.S.A.* **90**, 883 (1993); G. Gill, E. Pascal, Z. H. Tseng, R. Tjian, *ibid.* **91**, 192 (1994).
28. C.-M. Chiang and R. G. Roeder, *Peptide Res.* **6**, 62 (1993).
29. D. I. Chasman, J. Leatherwood, M. Carey, M. Ptashne, R. D. Kornberg, *Mol. Cell. Biol.* **9**, 4746 (1989).
30. M. A. Blamar and W. J. Rutter, *Science* **256**, 1014 (1992).
31. A. Hoffmann, C.-M. Chiang, R. G. Roeder, unpublished data.
32. A. J. Courey and R. Tjian, *Cell* **55**, 887 (1988).

33. We thank K. Hisatake for recombinant HA:230 baculovirus; J. L. Chen and R. Tjian for Sp1 proteins; R. Kageyama and S. Nakanishi for the human placental cDNA library; B. Cullen, Y.-S. Lin, F. Liu, H.-C. Liou, Y. Shi, and J.-B. Yoon for plasmids; A. Hoffmann (anti-TBP and anti-TAF_{II}20), M. Kretzschmar (anti-p50), E. Martinez (anti-YY1), P. Pognonec (anti-USF), S. Stevens (anti-TAF_{II}135), R. Takada (anti-TAF_{II}230, anti-TAF_{II}95, and anti-TAF_{II}80), and N. Tanese (anti-CTF1) for antibodies; S.-Y. Wu for constructing f:USF and f:50 expression plasmids and performing yeast two-hybrid analysis; X. Zhang for

preparing nuclear extracts; J. Huang for maintaining cell lines; E. Hendricks for assistance in generating polyclonal antibodies; H. Ge and Z. Wang for discussions about chromatography; and the protein sequencing facility of the Rockefeller University for synthesizing the FLAG peptide and performing protein microsequencing analysis. Supported by NIH and by grants from the Pew Trusts to Rockefeller University. C.-M.C. is a Helen Hay Whitney Foundation and Aaron Diamond Foundation postdoctoral fellow.

8 September 1994; accepted 29 November 1994

TECHNICAL COMMENTS

Paleotopography of Glacial-Age Ice Sheets

W. R. Peltier (1) presents a model that reconstructs the paleotopography of glacial-age ice sheets on the basis of sea level curves and the viscoelastic properties of the earth's crust and mantle. The model has profound implications because it suggests that the elevation of northern hemisphere glacial-age ice sheets was much lower than previously believed. The low topography has implications for atmospheric general circulation models of ice age climate. Furthermore, the model suggests that the glacial-age Antarctic Ice Sheet was significantly larger than today's.

Such models can now be tested more rigorously because of the advent of sea level curves that have high resolution and cover most of deglaciation. Before the late 1980s, most deglacial records covered only the very last portion of deglaciation and chronologies were established with ¹⁴C dating. In the late 1980s the development of thermal ionization mass spectrometric (TIMS) techniques for measuring ²³⁴U (2) and ²³⁰Th (3) provided the capability to obtain high-precision ²³⁰Th ages of coral skeletons (3). TIMS ²³⁰Th dates have advantages over ¹⁴C dates because they (i) have higher precision and (ii) do not require independent calibration. The advent of TIMS ²³⁰Th dating provided impetus for researchers to drill for deglacial sequences of corals, with the goal of obtaining long, high-resolution records of deglaciation.

Two sequences that cover most of deglaciation have been drilled and analyzed: the Barbados sequence (4), which covers the complete deglaciation, and the Papua New Guinea sequence (5, 6), which covers the last half of deglaciation. Peltier (1) used the Barbados sea level record to tune his model and tested model output against the Papua New Guinea record. Model output matched the Papua New Guinea record well, apparently supporting the model's validity.

However, Peltier (1) used depths for the

Papua New Guinea and Barbados data that were not corrected for tectonic uplift. The Barbados uplift rate is small, 0.34 m per thousand years (4), amounting to a correction of 7 m for the deepest portion of the core. Thus, the Barbados correction can be excluded without serious consequence. The model results disagree only slightly with the corrected Barbados record (Fig. 1). On the other hand, the uplift rate at the Papua New Guinea site is much larger. The rate of 1.9 m per thousand years is well known and documented (5-7), and amounts to a correction of more than 20 m for the oldest portion of the record (5, 6). Model results disagree with the corrected Papua New Guinea record (Fig. 1). Because the Barbados curve was used for tuning, the Papua New Guinea record is the only long independent sea level curve upon which to test model results. The inability of the model to

reproduce the Papua New Guinea curve would appear to cast doubt on other model results, including those related to the paleotopography of the glacial ice sheets. Thus, resolution of the discrepancy between the Papua New Guinea data and the modeling results is a central issue.

R. Lawrence Edwards

Minnesota Isotope Laboratory,
Department of Geology and Geophysics,
University of Minnesota,
Minneapolis, MN 55455, USA

REFERENCES

1. W. R. Peltier, *Science* **265**, 195 (1994).
2. J. H. Chen, R. L. Edwards, G. J. Wasserburg, *Earth Planet. Sci. Lett.* **80**, 241 (1986).
3. R. L. Edwards, J. H. Chen, G. J. Wasserburg, *ibid.* **81**, 175 (1987); R. L. Edwards, J. H. Chen, T.-L. Ku, G. J. Wasserburg, *Science* **236**, 1547 (1987).
4. R. G. Fairbanks, *Nature* **342**, 637 (1989); E. Bard, B. Hamelin, R. G. Fairbanks, A. Zindler, *ibid.* **345**, 405 (1990).
5. J. M. A. Chappell and H. A. Polach, *ibid.* **349**, 147 (1991).
6. R. L. Edwards *et al.*, *Science* **260**, 962 (1993).
7. J. M. A. Chappell, *Geol. Soc. Am. Bull.* **85**, 553 (1974); A. L. Bloom, W. S. Broecker, J. M. A. Chappell, R. K. Matthews, K. J. Mesollala, *Quat. Res.* **4**, 185 (1974); A. L. Bloom and N. Yonekura, in *Models in Geomorphology*, M. J. Woldenberg, Ed. (Allen & Unwin, Winchester, MA, 1985), pp. 140-154.
8. Sea level work supported by NSF grants EAR-8904705, ATM-8921760, and OCE-9402693.

28 July 1994; accepted 23 November 1994

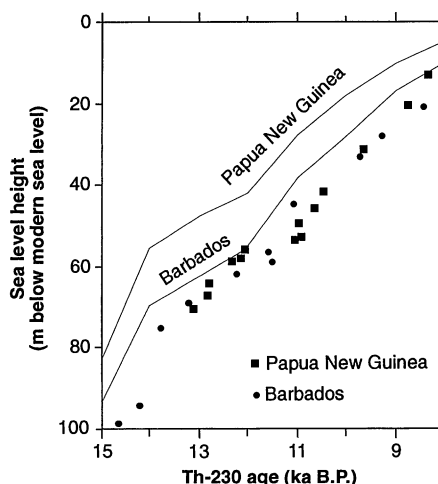


Fig. 1. Discrepancy between model results (1) and sea level data (4, 6). Deglacial sea level rise as recorded in Papua New Guinea [squares, (6)] and Barbados [circles, (4)] corals. Data points are corrected for tectonic uplift at each site. Curves represent sea level rise at each of the two localities, as predicted by Peltier's (1) model.

Response: I am grateful for having attention drawn to one of the secondary aspects of the work described in my article (1). My purpose was to advance a methodology whereby the continental ice sheets that existed at the Last Glacial Maximum (LGM) might be "weighed," even in absentia. The limited application of this methodology (1) was based on several assumptions, mainly that (i) the ice sheets could be safely assumed to be in isostatic equilibrium at LGM, (ii) the viscosity of the planetary mantle was approximately a function of radius only, and (iii) the records of relative sea level history based on coral sequences from Barbados and the Huon Peninsula of Papua New Guinea could be analyzed without making the usual correction for a presumed constant local rate of tectonic uplift. Edwards questions the reasonableness of (iii), given the extent to which the 0.34 mm year⁻¹ and 1.9 mm